RAPID COMMUNICATIONS

PHYSICAL REVIEW B VOLUME 39, NUMBER 16 1 JUNE 1989

Quantum dynamics of a pulsed spin system: Long-time behavior of semiclassical wave functions

K. Nakamura
*The James Franck Institute, The University of Chicago, Chicago, Illinois, 60637 and Fukuoka Institute of Technology, Higashi-ku, Fukuoka 811-02, Japan**

A. R. Bishop
Theoretical Division and Center for Nonlinear Studies, Los Alamos National Laboratory, Los Alamos, New Mexico 87545

A. Shudo
Department of Applied Physics, Waseda University, Shinjuku-ku, Tokyo 160, Japan
(Received 17 February 1989)

Semiclassical wave-function patterns in a pulsed spin system are examined in the post crossover-time regime. They show ergodic and nonergodic features possessed by the underlying classical dynamics. Local dimensions (i.e., singularities) of their probability density functions maintain enhanced fluctuations when the pulse strength lies in a transitional region leading to global chaos.

The quantum mechanics of classically chaotic systems constitutes a very active field of contemporary physics.[1,2] Considering quantum *dynamics*, the coherent structure of wave functions is greatly affected by quantum interference, leading to the suppression of anomalous diffusion features characteristic of chaos and eventually to the vanishing of Kolmogorov-Sinai entropy and of other characteristic exponents. If we examine a semiclassical regime, however, new phenomena can appear, not present in either the classical or quantum limit.[3] In particular, semiclassical wave-function patterns may exhibit several distinctive behaviors in a recurrent time regime beyond the crossover time t_c at which the classical and quantum correspondence breaks down. [In the case of hyperbolic fixed points of the corresponding classical motion, $t_c \sim (\text{Lyapunov exponent})^{-1} \times \ln(\hbar^{-1})$ (see, e.g., Berry and Balazs.[2])] But these behaviors have not so far been examined systematically; most previous studies on the dynamics of wave functions have concentrated on the time regime $t<t_c$.[2] For a study of longtime and semiclassical behaviors, quantum-large spin systems are especially advantageous because the finite dimensionality of their Hilbert space requires no artificial truncation of energy matrices.[4,5] Further, in the experiment of spin echoes in electron spin resonance, for instance, an assembly of spin-$\frac{1}{2}$ systems behaves coherently and effectively constitutes a single large quantum spin.

In this Rapid Communication, we examine the long-time behavior of wave functions in a periodically pulsed large quantum-spin system whose classical limit exhibits a transition from predominantly regular orbits to global chaos as the pulse strength is increased.[4] The effect of dissipation is omitted in the present treatment. We shall attempt to characterize wave-function patterns in terms of the singularity spectra $f(\alpha)$,[6] which has proven very useful recently in quantifying multifractal aspects of chaotic systems.

The quantum dynamics for our spin system with $\mathbf{S}=(S^x,S^y,S^z)$ is described by $i\hbar\dot{\Psi}=H\Psi$, where $H=H_0+\sum_{n=-\infty}^{\infty}V\delta(t-2\pi n)$ with $H_0=A(S^z)^2$ and $V=-\mu BS^x$. $A(>0)$ and $\mu B(>0)$ represent a planar anisotropy and pulse strength, respectively.[4] [Here we have chosen a convenient model Hamiltonian. One may make other choices, e.g., $H_0=AS^z$ and $V=-\mu BS^x \times\cos(\omega t)$, without changing the qualitative features of the results below.] We solve the above Schrödinger equation by rewriting it immediately in a matrix form; a set of eigenstates of S^z is chosen as basis kets. Then, the wave function Ψ just after the nth pulse is given by

$$\Psi(2\pi n+0)=\sum_{m=-S}^{S}C_m(2\pi n+0)\,|m\rangle\,,$$

with

$$\mathbf{C}(2\pi n+0)=\sum_{\alpha}\exp(-2\pi i n E_\alpha/\hbar)[\mathbf{X}_\alpha^\dagger\cdot\mathbf{C}_\alpha(+0)]\mathbf{X}_\alpha\,.$$

Here $\{E_\alpha\},\{\mathbf{X}_\alpha\}$ are quasienergies and quasieigenfunctions for the one-period propagator represented by the unitary matrix

$$\hat{U}=\exp[-(i/\hbar)\hat{V}]\exp[-(i/\hbar)2\pi\hat{H}_0]\,.$$

$\hat{V}$ and $\hat{H}_0$ are matrices for V and H_0, respectively.[4] The probability density function is given in terms of $SU(2S+1)$ coherent state representations as

$$P_n(\theta,\phi)=[(2S+1)/4\pi]\,|\langle\theta,\phi\,|\,2\pi n+0\rangle|^2\,,$$

where the first factor on the right-hand side is due to the normalization over the surface of a unit radius sphere. In the following, $A=1.0$ sets the energy unit. Further, we employ $S=128$ and choose $\hbar=1/\sqrt{S(S+1)}$ so that the observable spin magnitude maintains the scaled value for the classical spin vector, i.e., $\mathbf{S}^2=S(S+1)\hbar^2=1$.

In Fig. 1, very early stages $(n=1,2,3)$ of the temporal evolution of initially $(n=0)$ localized wave packets are shown. For a weak pulse $(\mu\tilde{B}\equiv\mu B/A=0.01)P_n(\theta,\phi)$

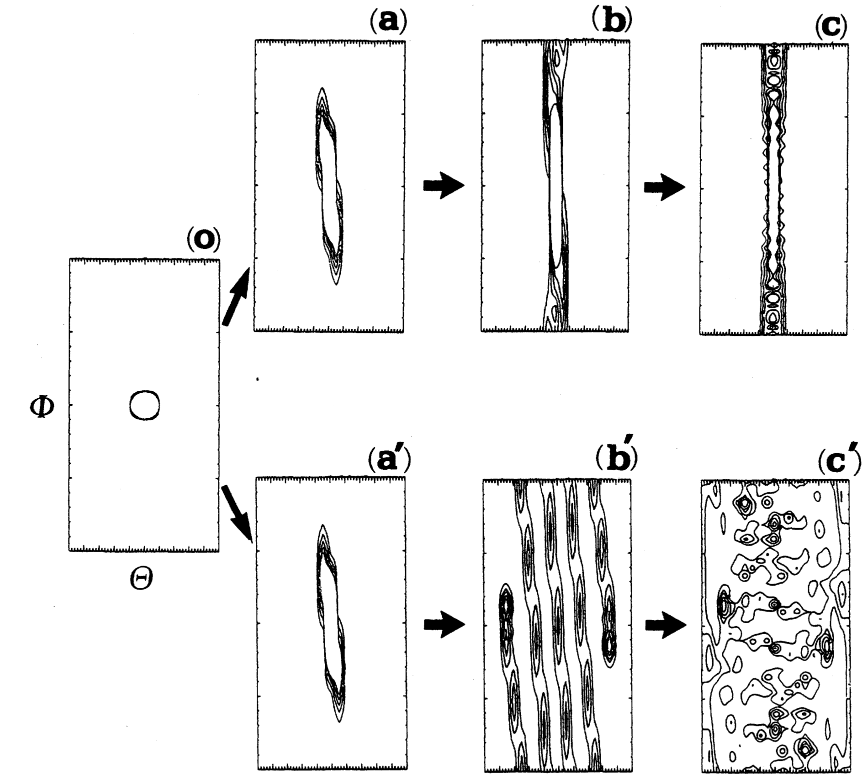

FIG. 1. Contour map for very early stages of $P_n(\theta,\phi)$: (o) Initial ($n=0$) wave packet; (a)–(c) time evolution for $\mu\tilde{B}=0.01$; (a′)–(c′) time evolution for $\mu\tilde{B}=1.0$. From the left, $n=1$, 2, and 3.

shows a simple unidirectional diffusion [see Figs. 1(a)–1(c)] corresponding to regular behavior in classical dynamics. [Note that investigation of classical dynamics indicates[4] the presence of two characteristic fields $\mu\tilde{B}_1 \cong 0.1$ and $\mu\tilde{B}_2 \cong 0.5$, where the fraction of chaotic trajectories increases strongly and the last Kol'mogorov-Arnol'd-Moser (KAM) torus disappears, respectively.] However, for a strong pulse ($\mu\tilde{B}=1.0$) remarkably isotropic and irregular diffusions begin after the period of "classical" stretching- and folding-type diffusion. Figure 1 also indicates $t_c=O(1)$ for both the $\mu\tilde{B}=0.01$ and 1.0 cases. The above results resemble a quantized version of abstract dynamical systems (e.g., C or K systems), in which wave functions have been reported to exhibit highly irregular patterns after stretching and folding.[7] Also, certain eigenstates were found with anomalous localization lengths. Because of the difference of wave-function representations between us and Ref. 7, however, it is difficult to make quantitative comparisons.

We now proceed to examine $P_n(\theta,\phi)$ in large n regions ($n=70$, 90, 110) (see Figs. 2). While the exact classical-quantum correspondence has been lost in this time region, these figures clearly maintain some images of the underlying classical dynamics: Figures 2(a)–2(c), 2(a′)–2(c′), and 2(a″)–2(c″) retain signatures of nonergodicity at $\mu\tilde{B}=0.01$, of partial egordicity at $\mu\tilde{B}=0.2$, and of complete ergodicity at $\mu\tilde{B}=1.0$, respectively.[8] In fact, localized regular structures with large amplitudes keep a quasiperiodic oscillation for $\mu\tilde{B}=0.01$ and fine structures with small amplitudes continue to occupy the global phase space for $\mu\tilde{B}=1.0$. For $\mu\tilde{B}=0.2$, fine structures continue to occupy a limited portion of phase space.

We now try to quantify $P_n(\theta,\phi)$ in terms of multifractals.[6] Since $P_n(\theta,\phi)$ is already normalized to unity in the θ-ϕ plane, the calculation of the singularity spectra $f(\alpha)$ is straightforward: for a linear scale l, we consider the square $l\times l$ mesh $A_i(l)$ around the position (θ,ϕ) and calculate

$$P_{n,i}(l)=\int_{(\theta,\phi)\subset A_i(l)} P_n(\theta,\phi)\sin\theta\, d\theta\, d\phi\,.$$

Summing $P^q_{n,i}(l)$ over all meshes, we obtain the partition function $\Gamma(q,l)$. The scaling property of $\Gamma(q,l)$ is then examined by changing l according to $l=l_0\times 2^m$ ($m=0,1,2,\dots$) with $l_0=O(S^{-1/2})$. The scaling exponents τ_q thus obtained are used to find $f(\alpha)$. It should be noted, however, that our numerical data $P_n(\theta,\phi)$ are reliable only to the order of 10^{-5}. Using them as inputs, we can obtain wide scaling regions for $\Gamma(q,l)$ in the case $q\geq 0$, but it is difficult to explore sufficiently wide scaling regions in the case $q<0$. So our analyses of $f(\alpha)$ below will be limited to the $q\geq 0$ case. This restriction does not prevent us from studying the general tendencies of fluctuations of singularities or local dimensions α. Figure 3 represents $f(\alpha)$ with $q\geq 0$ for several $\mu\tilde{B}$ values at a fixed time $n=90$. We find that fluctuations of α for $\mu\tilde{B}=0.01$

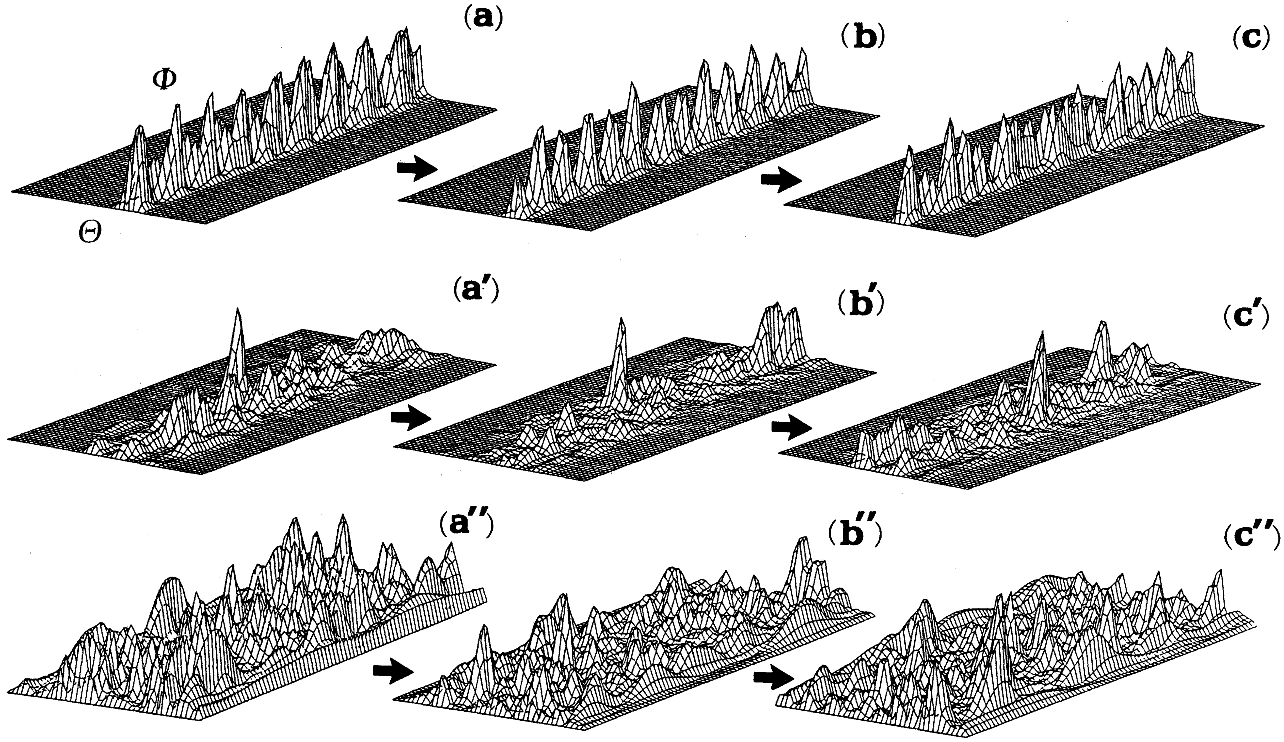

FIG. 2. Time evolution of three-dimensional profiles of $P_n(\theta,\phi)$ for $n \gg 1$: (a)–(c) $\mu\tilde{B}=0.01$; (a′)–(c′) $\mu\tilde{B}=0.2$; (a″)–(c″) $\mu\tilde{B}=1.0$. From the left, $n=70$, 90, and 110.

and 1.0 fall into a narrow range and those for $\mu\tilde{B}=0.2$ extend over a much wider range. The large fluctuation in the latter signifies the inhomogeneous distribution of measure $P_n(\theta,\phi)$ in Fig. 2(b′), which reflects the coexistence of classical KAM orbits and localized chaos in a transitional region leading to global chaos. This large fluctuation is reminiscent of the critical fluctuations at an equilibrium phase transition. The relatively small fluctuation for $\mu\tilde{B}=1.0$ signifies the uniform distribution of measures in Figs. 2(b″). (Note that the above enhanced fluctuations will not be observed in quantized K or C system[7] whose classical versions are homogeneously unstable and have neither KAM torii nor a transitional region.)

Using our data for $f(\alpha)$ with $q \geq 0$, we now estimate the effective range of fluctuations $\alpha^*_{\rm min} \leq \alpha \leq \alpha^*_{\rm max}$:$\alpha^*_{\rm max}$ and $\alpha^*_{\rm min}$ denote the value at which $f(\alpha)$ takes the maximum (i.e., fractal dimension) and the value at which $f(\alpha)$ takes $\frac{2}{3}$ times its maximum (an arbitrary choice). For $\mu\tilde{B}=0.2$ at $n=90$, for example, $\alpha^*_{\rm max}=1.98\pm0.02$ and $\alpha^*_{\rm min}=1.35\pm0.02$. (The error bars apply for $n<130$.) In Fig. 4, the time dependence of the effective ranges thus introduced are shown for the interval

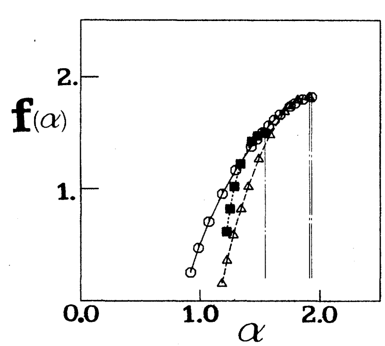

FIG. 3. $f(\alpha)$ in $q \geq 0$ regime at $n=90$. Squares, circles, and triangles correspond to $\mu\tilde{B}=0.01$, 0.2, and 1.0, respectively.

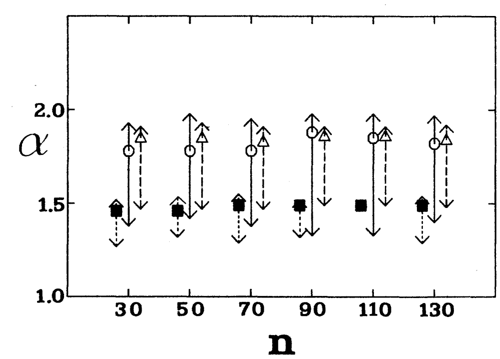

FIG. 4. Time evolution of effective range of $f(\alpha)$ (see text). Dotted, solid, and broken lines correspond to $\mu\tilde{B}=0.01$, 0.2, and 1.0, respectively. Symbols (■,○,△) in each range denote the fractal dimensions, i.e., peak values of $f(\alpha)$. [The range in the case of $\mu\tilde{B}=0.01$ at $n=110$ is suppressed because of an accidental narrowing of scaling regions which makes it difficult to obtain reliable $f(\alpha)$ values.]

$30 \leq n \leq -130$ steps of 20. The features in Fig. 3, which have now been quantified, are found to persist throughout the temporal evolution. Careful examinations indicate: (1) the effective range of α shows distinctive temporal variations for $\mu\tilde{B} = 0.2$; (2) on the other hand, it remains almost unchanged for $\mu\tilde{B} = 1.0$ (despite the absence of dissipation in the present system), which reflects a well-organized ergodicity in this case.

The mixing and ergodic features of classical chaos have helped to establish relationships with the formalism of equilibrium statistical mechanics.[9] In the field of quantum chaos, most of the literal definitions of classical chaos lose their significance. Nonetheless, we still find complicated behaviors in the quantum mechanical treatment of chaotic systems, as shown in this study. We believe that the characterization given here will be a vehicle for more profound understanding of these complexities.

In conclusion, despite the complete absence of classical and quantum correspondence, the longtime behavior of semiclassical wave functions maintains the ergodic and nonergodic features possessed by the underlying classical dynamics. The enhance fluctuation of their local dimensions in a transitional region leading to global chaos persists throughout the time evolution, which is reminiscent of critical fluctuations at an equilibrium phase transition.

We acknowledge valuable discussions with M. Feingold, P. Gaspard, A. Libchaber, S. A. Rice, and N. Saitô.

*Permanent address.

[1]See, e.g., *Quantum Chaos and Statistical Nuclear Physics,* edited by T. H. Seligman and H. Nishioka (Springer, Berlin, 1986).

[2]G. Casati *et al.*, in *Stochastic Behavior in Classical and Quantum Hamiltonian Systems,* edited by G. Casati and J. Ford (Springer, Berlin, 1979); M. V. Berry and N. L. Balazs, J. Phys. A **12**, 625 (1979); T. Hogg and B. A. Huberman, Phys. Rev. Lett. **48**, 711 (1982); D. R. Grempel, S. Fishman, and R. E. Prange, *ibid.* **53**, 1212 (1984); S. Chang and K. Shi, *ibid.* **55**, 269 (1985).

[3]M. V. Berry, Proc. R. Soc. London Ser. A **413**, 183 (1987).

[4]K. Nakamura, Y. Okazaki, and A. R. Bishop, Phys. Rev. Lett. **57**, 5 (1986). The analysis in this reference was restricted to individual quasieigenfunctions.

[5]For studies on quantum dynamics of nonintegrable spin systems, see also: G. Müller, Phys. Rev. A **34**, 3345 (1986); H. Frahm and H. J. Mikeska, Z. Phys. **65**, 249 (1986); M. Kus, R. Scharf, and F. Haake, *ibid.* B **66**, 129 (1987).

[6]T. Halsey *et al.*, Phys. Rev. A **33**, 1141 (1986); L. Pietronero and A. P. Siebesma, Phys. Rev. Lett. **57**, 1098 (1986); M. C. Gutzwiller and B. B. Mandelbrot, *ibid.* **60**, 673 (1988).

[7]N. L. Balazs and A. Voros, Europhys. Lett. **4**, 1089 (1987); and Ann. Phys. (N.Y.) (to be published).

[8]Here we do not consider the problem of formulating quantum ergodicity. The formulation of ergodic theorems in quantum mechanics is a longstanding problem and many studies have been made around von Neumann's theorem on "weak convergence" for macro-observables. An interesting review is given in P. Pechukas, J. Phys. Chem. **88**, 4823 (1984).

[9]R. Bowen, *Equilibrium States and the Ergodic Theory of Anosov Diffeomorphisms* (Springer, Berlin, 1975); D. Ruelle, *Thermodynamic Formalism* (Addison-Wesley, Reading, MA, 1978).